Effects of σ^* and ϕ on the proto-neutron star PSR J0348+0432 *

Bin Hong(洪斌)[1] Zhong-Zhou Ren(任中洲)[1,2;1)]

[1] Department of Physics, Nanjing University, Nanjing 210008, China
[2] School of Physics Science and Engineering，Tongji University, Shanghai 200092, China

Abstract: The influence of σ^* and ϕ on the proto-neutron star (PNS) PSR J0348+0432 is described by the relativistic mean field theory (RMFT) through choosing effective coupling constants. We use an entropy per baryon $S=1$ to describe the thermal effects on PSR J0348+0432 in this work and compare this PNS with and without σ^*, ϕ. These effects include the particle number distribution, mass-radius relation, moment of inertia and surface gravitational redshift. The PNS PSR J0348+0432 with σ^* and ϕ has more nucleons and will push forward the threshold for the appearance of the hyperons. The mass-radius relations are ($2.010M_\odot$, 12.6520 km) with σ^* and ϕ and ($2.010M_\odot$, 12.6170 km) without σ^* and ϕ. The moments of inertia corresponding to PNS PSR J0348+0432 are ($2.010M_\odot$, 1.510×10^{45} g·cm^2) and ($2.010M_\odot$, 1.559×10^{45} g·cm^2) respectively, and the surface gravitational redshifts are ($2.010M_\odot$, 0.3747) and ($2.010M_\odot$, 0.3701) respectively. With the help of these calculations, we study the restriction of σ^* and ϕ on the interactions between baryons in the PNS core.

Keywords: proto-neutron star, PSR J0348+0432, strange mesons

PACS: 26.60.-c, 26.60.Kp, 21.65.Jk **DOI:** 10.1088/1674-1137/42/8/084105

1 Introduction

Neutron stars are compact stars, and exist under extreme physical conditions. Recently, the gravitational wave event GW170817 was detected from a binary neutron star inspiral, making neutron stars a hot research topic [1, 2]. It is meaningful to study them theoretically with various methods. In particular, a mass of $1.97\pm0.04M_\odot$ for the massive neutron star PSR J1614-2230 was obtained using the Shapiro delay method by Demorest et al in 2010 [3], and a mass of $2.01\pm0.04M_\odot$ was measured for PSR J0348+0432 by a combination of radio timing and precise spectroscopy of the white dwarf companion by Antoniadis et al in 2013 [4]. So far, these are the only two massive neutron stars with mass exceeding $2M_\odot$ to be observed. A stiffer equation of state is then needed to support the maximum mass of the neutron star. Some theoretical calculations and analytical approaches have been identified to support these observations [5–8].

Relativistic mean field theory (RMFT) has been used to describe neutron stars in many studies [9, 10], considering the baryon-baryon interaction through the exchange of σ,ρ,ω mesons. However, if we consider an additional interaction which couples strongly to strange baryons, the σ^* and ϕ mesons should be included [11, 12].

Many studies have discussed neutron stars based on zero temperature [13–15]. For example, the work by Xian-Feng Zhao [16] discusses the effect of σ^* and ϕ on the surface gravitational redshift of PSR J0348+0432 and gives a meaningful result. However, the result was obtained for zero temperature. A cold neutron star is a kind of evolutionary outcome of a PNS, which is formed after an enormous supernova. So the properties and structure of a PNS should be considered, but little attention has been paid to this topic.

In this paper, we investigate the influence of σ^* and ϕ mesons on the massive neutron star PSR J0348+0432 at finite entropy using RMFT. The paper is organized as follows. In Section 2, we give the complete form of relativistic mean field of hadron interactions at finite entropy including the σ^* and ϕ mesons. In Section 3, details are given of the selection of hyperon coupling constants. In Section 4, some calculation results of the effect of σ^* and ϕ mesons on the massive PNS PSR J0348+0432 are given. In Section 5, a summary is presented.

2 Basics of relativistic mean field theory in proto-neutron stars

RMFT is an effective field theory dealing with hadron-hadron interactions [15–20]. The interactions

Received 3 May 2018, Published online 9 July 2018

∗ Supported by National Natural Science Foundation of China (11535004, 11761161001) and the National Major State Basic Research and Development Program of China (2016YFE0129300)

1) E-mail: zren@nju.edu.cn, zren@tongji.edu.cn

proceed by exchanging σ,ω,ρ mesons, where σ is a scalar meson, ω is a vector meson and ρ is the vector-isospin meson. The Lagrangian density is described by [21]:

$$\begin{aligned}\mathcal{L}_0 =& \sum_{\rm B}\overline{\Psi}_{\rm B}(i\gamma_\mu\partial^\mu-m_{\rm B}+g_{\sigma{\rm B}}\sigma-g_{\omega{\rm B}}\gamma_\mu\omega^\mu\\&-\frac{1}{2}g_{\rho{\rm B}}\gamma_\mu\tau\cdot\rho^\mu)\Psi_{\rm B}+\frac{1}{2}(\partial_\mu\sigma\partial^\mu\sigma-m_\sigma^2\sigma^2)\\&-\frac{1}{4}\omega_{\mu\nu}\omega^{\mu\nu}+\frac{1}{2}m_\omega^2\omega_\mu\omega^\mu-\frac{1}{4}\rho_{\mu\nu}\cdot\rho^{\mu\nu}+\frac{1}{2}m_\rho^2\rho_\mu\cdot\rho^\mu\\&-\frac{1}{3}g_2\sigma^3-\frac{1}{4}g_3\sigma^4+\sum_{\rm l=e,\mu}\overline{\Psi}_{\rm l}(i\gamma_\mu\partial^\mu-m_{\rm l})\Psi_{\rm l}. \end{aligned}\tag{1}$$

In this work, an additional scalar meson σ^* and an additional vector meson ϕ are considered. We need to know their interaction with hyperons, which can be described by the Lagrangian density $\mathcal{L}'$ [22]

$$\begin{aligned}\mathcal{L}' =& \sum_{\rm B}\overline{\Psi}_{\rm B}(g_{\sigma^*{\rm B}}\sigma^*-g_{\phi{\rm B}}\gamma_\mu\phi^\mu)\Psi_{\rm B}\\&+\frac{1}{2}(\partial_\mu\sigma^*\partial^\mu\sigma^*-m_{\sigma^*}^2\sigma^{*2})\\&-\frac{1}{4}\phi_{\mu\nu}\phi^{\mu\nu}+\frac{1}{2}m_\phi^2\phi_\mu\phi^\mu, \end{aligned}\tag{2}$$

where B, l denote the octet baryons and leptons respectively. The total Lagrangian density is expressed by $\mathcal{L}=\mathcal{L}_0+\mathcal{L}'$.

According to statistical thermodynamics:

$$\begin{aligned}\ln Z_{\rm B,l} =& \sum_{\rm B,l}\frac{2J_{\rm B,l}+1}{2\pi^2}\int_0^\infty k^2{\rm d}k\{\ln[1+{\rm e}^{-(\varepsilon_{\rm B,l}(k)-\mu_{\rm B,l})/T}]\\&+\frac{V}{T}<\mathcal{L}>, \end{aligned}\tag{3}$$

where J and μ are the spin quantum number and the chemical potential. $Z=\mathrm{Tr}\{\exp[-(\hat{H}-\mu\hat{N})/T]\}$ is the grand partition function. The energy density, pressure and particle population density are related to it as:

$$\varepsilon = \frac{T^2}{V}\frac{\partial\ln Z}{\partial T}+\mu n, \tag{4}$$

$$P = \frac{T}{V}\ln Z, \tag{5}$$

$$n = \frac{T}{V}\frac{\partial\ln Z}{\partial\mu}. \tag{6}$$

The entropy per baryon of proto-neutron star matter can be expressed as $S_{\rm B}=P_{\rm B}+\varepsilon_{\rm B}-\sum_{i=B}\mu_{\rm i}\rho_{\rm i}$ for baryons and $S_{\rm l}=P_{\rm l}+\varepsilon_{\rm l}-\sum_{i=l}\mu_i\rho_i$ for leptons [5, 23].

The additional conditions of a neutron star system are charge neutrality and chemical potential equilibrium, which are as follows:

$$\sum_{\rm B,l}\frac{2J_{\rm B,l}+1}{2\pi^2}q_{\rm B,l}\int_0^\infty k^2n_{\rm B,l}(k){\rm d}k=0, \tag{7}$$

$$\mu_i=b_i\mu_n-q_i\mu_e, \tag{8}$$

where $n_{\rm i}(k)=1/(1+\exp[(\varepsilon_{\rm i}(k)-\mu_{\rm i})/T])({\rm i}={\rm B,l})$ denotes the Fermi distribution function.

Therefore, the energy density and pressure of a proto-neutron star under RMFT are as follows:

$$\begin{aligned}\varepsilon =& \frac{1}{3}g_2\sigma^3+\frac{1}{4}g_3\sigma^4+\frac{1}{2}m_\sigma^2\sigma^2+\frac{1}{2}m_\omega^2\omega_0^2+\frac{1}{2}m_\rho^2\rho_{03}^2+\frac{1}{2}m_{\sigma^*}^2\sigma^{*2}+\frac{1}{2}m_\phi^2\phi_0^2\\&+\sum_{\rm B}\frac{2J_{\rm B}+1}{2\pi^2}\int_0^\infty\sqrt{k^2+(m^*)^2}(\exp[(\varepsilon_{\rm B}(k)-\mu_{\rm B})/T]+1)^{-1}k^2{\rm d}k\\&+\sum_{\rm l}\frac{2J_{\rm l}+1}{2\pi^2}\int_0^\infty\sqrt{k^2+m_{\rm l}^2}(\exp[(\varepsilon_{\rm l}(k)-\mu_{\rm l})/T]+1)^{-1}k^2{\rm d}k, \end{aligned}\tag{9}$$

$$\begin{aligned}P =& -\frac{1}{3}g_2\sigma^3-\frac{1}{4}g_3\sigma^4-\frac{1}{2}m_\sigma^2\sigma^2+\frac{1}{2}m_\omega^2\omega_0^2+\frac{1}{2}m_\rho^2\rho_{03}^2-\frac{1}{2}m_{\sigma^*}^2\sigma^{*2}+\frac{1}{2}m_\phi^2\phi_0^2\\&+\frac{1}{3}\sum_{\rm B}\frac{2J_{\rm B}+1}{2\pi^2}\int_0^\infty\frac{k^2}{\sqrt{k^2+(m^*)^2}}(\exp[(\varepsilon_{\rm B}(k)-\mu_{\rm B})/T]+1)^{-1}k^2{\rm d}k\\&+\frac{1}{3}\sum_{\rm l}\frac{2J_{\rm l}+1}{2\pi^2}\int_0^\infty\frac{k^2}{\sqrt{k^2+m_{\rm l}^2}}(\exp[(\varepsilon_{\rm l}(k)-\mu_{\rm l})/T]+1)^{-1}k^2{\rm d}k, \end{aligned}\tag{10}$$

where $m^*=m_{\rm B}-g_{\sigma{\rm B}}\sigma-g_{\sigma^*{\rm B}}\sigma^*$ denotes the effective mass of baryons.

The mass and the radius of a neutron star can be calculated by the Tolman- Oppenheimer-Volkoff equation [24]:

$$\frac{{\rm d}p}{{\rm d}r}=-\frac{(p+\varepsilon)(M+4\pi r^3p)}{r(r-2M)}, \tag{11}$$

$$M(r)=4\pi\int_0^r \varepsilon r^2 \mathrm{d}r. \tag{12}$$

The moment of inertia of a neutron star is expressed as follows: [5, 25]:

$$I\equiv\frac{J}{\Omega}=\frac{8\pi}{3}\int_0^R r^4 \mathrm{e}^{-\nu(r)}\frac{\bar{\omega}(r)}{\Omega}\frac{(\varepsilon(r)+P(r))}{\sqrt{1-2GM(r)/r}}\mathrm{d}r, \tag{13}$$

J and Ω denote the angular momentum and the angular velocity respectively, and $\nu(r)$ is expressed as:

$$\nu(r) = -G\int_r^R \frac{(M(r)+4\pi x^3 P(x))}{x^2(1-2GM(x)/x)}\mathrm{d}x + \frac{1}{2}\ln\left(1-\frac{2GM}{R}\right). \tag{14}$$

We simply define $\tilde{\omega}(r)\equiv\bar{\omega}(r)/\Omega$ which satisfies the differential equation (15) as well as the boundary conditions (16-17):

$$\frac{\mathrm{d}}{\mathrm{d}r}\left(r^4 j(r)\frac{\mathrm{d}\widetilde{\omega}(r)}{\mathrm{d}r}\right)+4r^3\frac{\mathrm{d}j(r)}{\mathrm{d}r}\widetilde{\omega}(r)=0, \tag{15}$$

$$\widetilde{\omega}'(0)=0, \tag{16}$$

$$\widetilde{\omega}(R)+\frac{R}{3}\widetilde{\omega}'(R)=1. \tag{17}$$

Here,

$$j(r)=\begin{cases}\mathrm{e}^{-\nu(r)}\sqrt{1-2GM(r)/r} & r\leqslant R,\\ 1 & r>R.\end{cases} \tag{18}$$

The surface gravitational redshift of a star satisfies the relation [26, 27]:

$$z=\left(1-\frac{2GM}{c^2R}\right)^{-1/2}-1. \tag{19}$$

3 Coupling parameters

The RMFT model is based on the coupling constants of nucleons and hyperons. The nucleon coupling constants can be determined in the vicinity of the saturation properties of nuclear matter [28], and the hyperon coupling constants can be calculated by the hyper-nuclear potential well depth. In this work, we select the coupling parameter sets GL85 and GL97 listed in Table 1 and Table 2 [22].

Table 1. The GL85 coupling parameter sets.

m/MeV	m_σ/MeV	m_ω/MeV	m_ρ/MeV	g_σ	g_ω	g_ρ
939	500	782	770	7.9955	9.1698	9.7163
g_2/fm^{-1}	g_3	ρ_0/fm^{-3}	(B/A)/MeV	K/MeV	$a_{\rm sym}$/MeV	m^*/m
10.07	29.262	0.145	15.95	285	36.8	0.77

Table 2. The GL97 coupling parameter sets.

m/MeV	m_σ/MeV	m_ω/MeV	m_ρ/MeV	g_σ	g_ω	g_ρ
939	500	782	770	7.9835	8.7	8.5411
g_2/fm^{-1}	g_3	ρ_0/fm^{-3}	(B/A)/MeV	K/MeV	$a_{\rm sym}$/MeV	m^*/m
20.966	-9.835	0.153	16.3	240	32.5	0.78

We define the ratios: $x_{\sigma\mathrm{H}}=g_{\sigma\mathrm{H}}/g_\sigma=x_\sigma$,$x_{\omega\mathrm{H}}=g_{\omega\mathrm{H}}/g_\omega=x_\omega$,$x_{\rho\mathrm{H}}=g_{\rho\mathrm{H}}/g_\rho=x_\rho$, where H represents hyperons (Λ,Σ and Ξ). The relation of x_σ and x_ω must strictly satisfy the equation: [29]:

$$U_{\mathrm{H}}^{\mathrm{N}}=x_\omega(g_\omega/m_\omega)^2\rho_0-x_\sigma(m-m^*), \tag{20}$$

We select the values of hyper-nuclear potential well depth as $U_\Lambda^{\mathrm{N}}=-30$ MeV, $U_\Sigma^{\mathrm{N}}=+30$ MeV and $U_\Xi^{\mathrm{N}}=-15$ MeV respectively. [30–35]:

Reference [36] points out that the value of x_ω should be restricted in the range from 1/3 to 1. In this work, we select x_σ=0.4, 0.5, 0.6, 0.7, 0.8, 0.9, 1.0. For each x_σ, x_ω will be obtained according to the hypernuclear potential depth in nuclear matter $U_{\mathrm{H}}^{\mathrm{N}}$, as shown in Fig. 1 and Fig. 2. The calculations indicate that x_ω should be restricted to a narrow area depicted by the grid.

From the SU(6) symmetry, we can obtain the values of $x_{\rho\Lambda}$,$x_{\rho\Sigma}$ and $x_{\sigma\Xi}$: [37]

$$x_{\rho\Lambda}=0, \qquad x_{\rho\Sigma}=2, \qquad x_{\sigma\Xi}=1. \tag{21}$$

The hyperon-hyperon parameters through exchanging the strange scalar meson (σ^*) and strange vector meson (ϕ) can be selected as follows.

For the vector meson ϕ, according to the quark model relationships, the coupling parameters yield $2g_{\phi\Lambda}=2g_{\phi\Sigma}=g_{\phi\Xi}=-\frac{2\sqrt{2}}{3}g_\omega$.

For the scalar meson σ^*, we can use the $\sigma^*(975)$ meson mass which has been observed, but see purely phe-

nomenologically that it couples with hyperons so as to satisfy the potential well depths $U_{\Sigma}^{(\Xi)} \approx U_{\Lambda}^{(\Xi)} \approx U_{\Xi}^{(\Xi)} \approx 2U_{\Lambda}^{(\Lambda)} \approx 2U_{\Sigma}^{(\Lambda)} = 40$ MeV. This yields $g_{\sigma^*\Lambda}/g_{\sigma} = g_{\sigma^*\Sigma}/g_{\sigma} = 0.69$, $g_{\sigma^*\Xi}/g_{\sigma} = 1.25$ [12].

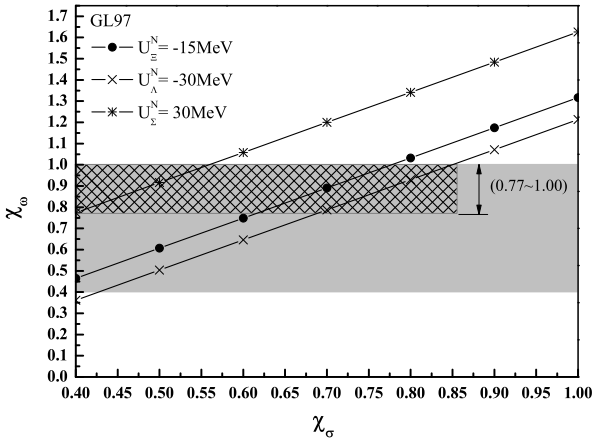

Fig. 1. The relation of x_σ and x_ω according to the the hypernuclear potential depth in nuclear matter $U_{\rm H}^{\rm N}$ with GL97.

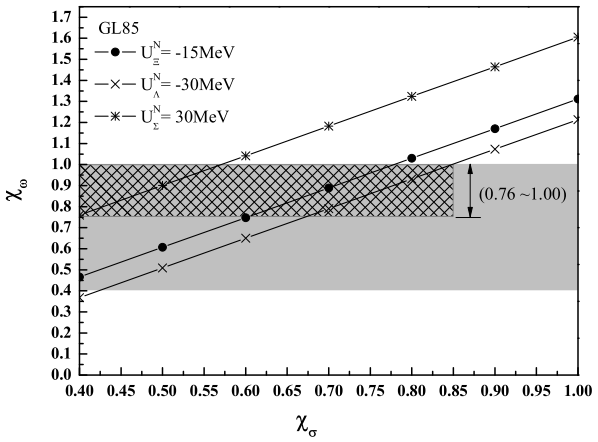

Fig. 2. The relation of x_σ and x_ω according to the the hypernuclear potential depth in nuclear matter $U_{\rm H}^{\rm N}$ with GL85.

4 Discussion

4.1 Mass and radius

Now, we calculate the mass of a protoneutron star without considering σ^* and ϕ. The neutrino effect may allow specification of the star characteristics in the interior, and the work by X. L. Mu et al. has given an interesting discussion of the contribution of neutrinos [38]. In this work, we do not consider the neutrino concentration, and select the entropy per baryon only to emphasize the thermal effect. In this work we select the entropy per baryon to be 1. Figure 1 gives that x_ω is 0.77 to 1.0, so we select the extreme value of x_ω=1.0. The maximum mass calculated is $1.9624M_\odot$, which cannot describe the PSR J0348+0348, whose mass is $2.0100M_\odot$. So, the GL97 parameter set may not give a perfect description of maximum protoneutron stars. Similarly, Fig. 2 gives that x_ω is in the range 0.76 to 1, and we use the same method to select the value of x_ω with GL85. For x_ω=1.0, 0.9, 0.8, and 0.76, the maximum mass is $2.1076M_\odot$, $2.0507M_\odot$, $1.9691M_\odot$, and $1.9294M_\odot$, respectively. Clearly, x_ω in the range between 0.8 and 0.9 can give the mass of $2.0100M_\odot$. First, we select x_ω=0.85 and get a maximum mass of $2.0126M_\odot$, which is bigger than $2.01M_\odot$. We select x_ω=0.84 and get a maximum mass of $2.0041M_\odot$, which is smaller than $2.01M_\odot$. Then, we select x_ω=0.845 and get a maximum mass of $2.0086M_\odot$. So we can restrict the value of x_ω to between 0.845 and 0.85. For x_ω=0.846, 0.847, 0.848, and 0.849, the maximum masses are $2.0092M_\odot$, $2.0100M_\odot$, $2.0112M_\odot$, and $2.0118M_\odot$, respectively. The calculations are shown in Fig. 3 and Table 3. We finally get the hyperon coupling constants $x_{\omega\Xi}$=$x_{\omega\Sigma}$=$x_{\omega\Lambda}$=0.847, corresponding to $x_{\sigma\Xi}$=0.670, $x_{\sigma\Sigma}$=0.462, $x_{\sigma\Lambda}$=0.740, and $x_{\rho\Lambda}$=0, $x_{\rho\Sigma}$=2, $x_{\sigma\Xi}$=1, from which we get that the maximum mass of a PNS is $2.0100M_\odot$ without considering σ^* and ϕ.

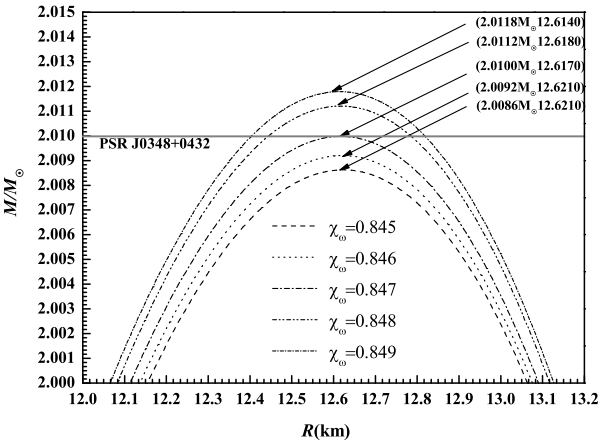

Fig. 3. Maximum neutron star mass of PNS as a function of radius for different x_ω without considering σ^* and ϕ.

Table 3. Maximum masses for different values of x_ω, without σ^* and ϕ.

x_ω	$M_{\rm max}$	x_ω	$M_{\rm max}$	x_ω	$M_{\rm max}$
1.0	$2.1076M_\odot$			0.845	$2.0086M_\odot$
0.9	$2.0507M_\odot$	0.85	$2.0126M_\odot$	0.846	$2.0092M_\odot$
0.8	$1.9691M_\odot$	0.84	$2.0041M_\odot$	**0.847**	$\mathbf{2.0100}M_\odot$
0.76	$1.9294M_\odot$			0.848	$2.0112M_\odot$
				0.849	$2.0018M_\odot$

When the σ^* and ϕ mesons are taken into account, our aim is also to get the maximum mass of a PNS corresponding to PSR J0348+0432. We select the value

of x_ω=1.0, 0.9, 0.8, and 0.76 according to Fig. 2. The maximum mass is $2.0998M_\odot$, $2.0449M_\odot$, $1.9376M_\odot$, and $1.8919M_\odot$ respectively and x_ω between 0.8 and 0.9 can give the mass of $2.01M_\odot$ by the same method above. First, we select x_ω=0.85 and get the maximum mass $1.9881M_\odot$, which is smaller than $2.0100M_\odot$. Then, we select x_ω=0.86, 0.87, 0.88, and 0.89, and get the maximum masses $1.9975M_\odot$, $2.0067M_\odot$, $2.0156M_\odot$, and $2.0242M_\odot$, respectively. On the basis of these results, we select the value of x_ω=0.875, which gives a maximum mass of $2.0112M_\odot$ and is bigger than $2.0100M_\odot$. So it is clear that we can restrict the value of x_ω to between 0.87 and 0.875. For x_ω=0.874, 0.873, 0.872, and 0.871, the maximum masses are $2.0100M_\odot$, $2.0093M_\odot$, $2.0085M_\odot$, and $2.0076M_\odot$, respectively. The calculations are shown in Fig. 4 and Table 4. We finally get the hyperon coupling constants $x_{\omega\Xi}$=$x_{\omega\Sigma}$=$x_{\omega\Lambda}$=0.874, corresponding to $x_{\sigma\Xi}$=0.689,$x_{\sigma\Sigma}$=0.481, $x_{\sigma\Lambda}$=0.759, and $x_{\rho\Lambda}$=0, $x_{\rho\Sigma}$=2,$x_{\sigma\Xi}$=1, from which we get that the maximum mass of a PNS is $2.0100M_\odot$ with σ* and ϕ taken into consideration.

As a result, we get two sets of hyperon coupling constants to describe the PNS PSR J0348+0432 by GL85 with and without considering σ* and ϕ. They are shown in Table 5. Figure 3 shows that the PNS PSR J0348+0432 has its radius at 12.617 km without the σ* and ϕ. When the σ* and ϕ are taken into account, the radius is 12.652 km, as shown by Fig. 4, which is bigger than the radius without considering σ* and ϕ.

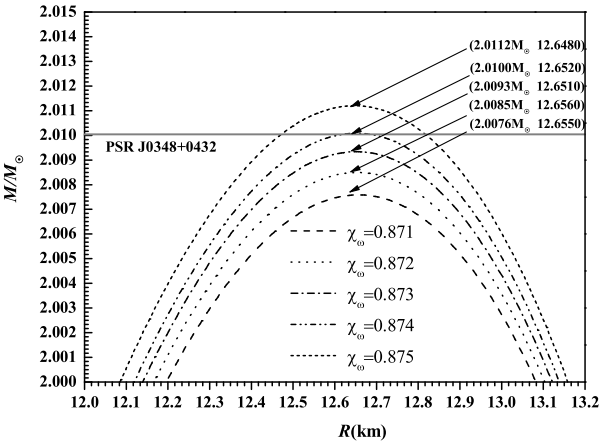

Fig. 4. Maximum neutron star mass of PNS as a function of radius for different x_ω with σ* and ϕ taken into consideration.

Table 4. Maximum masses for different values of x_ω, with σ* and ϕ.

x_ω	$M_{\max}$	x_ω	$M_{\max}$	x_ω	$M_{\max}$
1.0	$2.0098M_\odot$	0.85	$1.9881M_\odot$	0.871	$2.0076M_\odot$
0.9	$2.0449M_\odot$	0.86	$1.9975M_\odot$	0.872	$2.0085M_\odot$
0.8	$1.9376M_\odot$	0.87	$2.0067M_\odot$	0.873	$2.0093M_\odot$
0.76	$1.8919M_\odot$	0.88	$2.0156M_\odot$	**0.874**	$\mathbf{2.0100M_\odot}$
		0.89	$2.0242M_\odot$	0.875	$2.0112M_\odot$

Table 5. Two sets of hyperon coupling constants describing the PNS PSR J0348+0432. CASE1 is the case without σ* and ϕ and CASE2 is that with σ* and ϕ.

	$x_{\omega\Xi}$	$x_{\omega\Sigma}$	$x_{\omega\Lambda}$	$x_{\sigma\Xi}$	$x_{\sigma\Sigma}$	$x_{\sigma\Lambda}$	$x_{\rho\Xi}$	$x_{\rho\Sigma}$	$x_{\rho\Lambda}$
CASE1	0.847	0.847	0.847	0.670	0.462	0.740	1	2	0
CASE2	0.874	0.874	0.874	0.689	0.481	0.759	1	2	0

These results show that σ* and ϕ lead to increased radius, so the radius of the massive PNS PSR J0348+0432 with σ* and ϕ considered is bigger than that without σ* and ϕ considered. However, the difference is small.

4.2 Composition

Now we illustrate the particle (leptons, nucleons and hyperons) distributions of PNS PSR J0348+0432 for the case discussed in the text. Neutron star matter is not purely neutrons, as was first proposed. In the surface part of the star, nucleons are the dominant species, but in the inner part they are by no means dominant. Due to the uncertainty about the inner constitution, different hypothetical models will give different matter compositions. In this work, we consider the hyperons and the relative populations of various particles in PNS PSR J0348+0432 as described in Fig. 5. In this work, we select the GL85 parameter set, which give the nuclear saturation density at 0.145 fm^{-3}(ρ_0). In the neutron star interior the nucleons will convert to hyperons when the density exceeds the nuclear saturation density through the strong interaction. We can see the first hyperon to appear in the hadronic matter is Λ at 0.248 fm^{-3}($1.71\rho_0$), no matter whether or not the σ* and ϕ are considered. The next hyperon is Σ^-, appearing almost simultaneously around 0.399 fm^{-3} in both cases. However, the density at which Σ^0 appears is about 0.661 fm^{-3} with σ* and ϕ, and 0.721 fm^{-3} without σ* and ϕ. The Σ^+ appears at about 0.670 fm^{-3} with σ* and ϕ, and at 0.681 fm^{-3} without σ* and ϕ. For the hyperon Ξ, the density at which it appears is about 1.140 fm^{-3} with σ* and ϕ,

and 1.360 fm^{-3} without σ^* and ϕ. With σ^* and ϕ, the Ξ^0 appears at about 1.440 fm^{-3}, but without σ^* and ϕ, the Ξ^0 appears at a higher density which is not depicted in the figure.

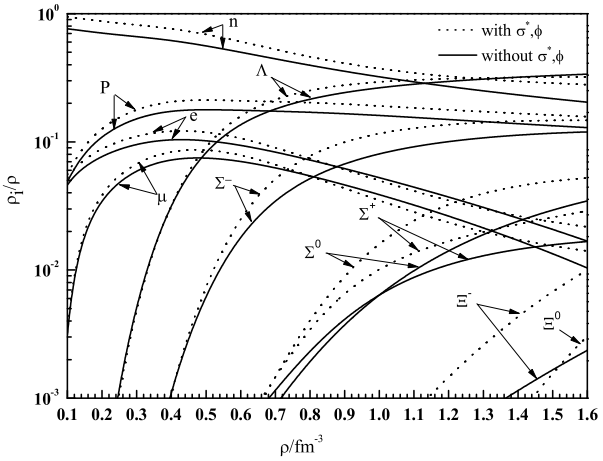

Fig. 5. Population of various particles in PNS PSR J0348+0432 with and without considering σ^* and ϕ.

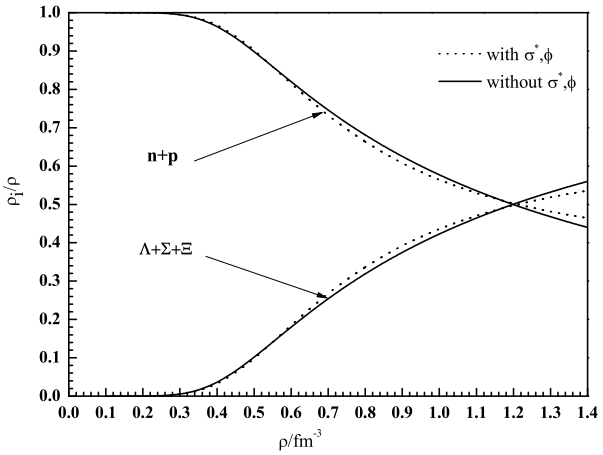

Fig. 6. Population of nucleon and hyperon as a function of baryon density in PNS PSR J0348+0432 with and without considering σ^* and ϕ.

These results show that in the context of considering σ^* and ϕ in PNS PSR J0348+0432, the threshold for the appearance of the hyperons will be pushed forward compared to that without considering σ^* and ϕ.

The population of nucleons (n,p) and hyperons (Λ,Σ,Ξ) as a function of baryon density is shown in Fig. 6. It clearly shows that when the hyperons appear, the number of nucleons decreases. The number of hyperons exceeds the number of nucleons at 1.199 fm^{-3}($8.27\rho_0$) without σ^* and ϕ included. We call this density the transition density, where the hyperons start to play an important role in the neutron star interior, and therefore the canonical neutron star converts to a hyperon star. When we consider σ^* and ϕ in the PNS PSR J0348+0432, the transition density appears at 1.211 fm^{-3}($8.35\rho_0$).

The field strengths of various mesons are shown in Fig. 7. Here, when considering σ^* and ϕ in PNS PSR J0348+0432, ω gives the stronger field strength while σ and ρ give the weaker field strength. We also distinctly see from Fig. 7 that the field strength of σ^* is larger than the field strength of ϕ, and both increase with the baryon density. In RMFT, the scalar mesons σ and σ^* provide attraction, and the vector mesons ω and ϕ provides repulsion. When considering σ^* and ϕ, because the attraction provided by σ^* is larger than the repulsion provided by ϕ, it leads to a stiffer equation of state.

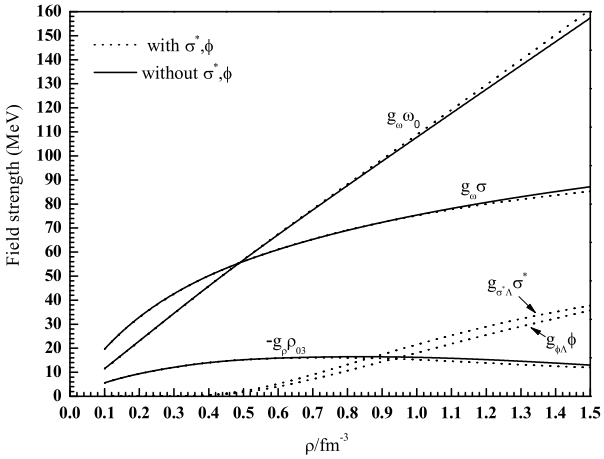

Fig. 7. Field strengths of various mesons in PNS PSR J0348+0432 with and without considering σ^* and ϕ.

4.3 Moment of inertia and surface gravitational redshift

With the equations of state obtained by solving the TOV equation, we have got the mass and radius shown in Fig. 3 and Fig. 4. With Eqs. (13-19), the moment of inertia and surface gravitational redshift can be found.

The profile of moment of inertia in a massive PNS for the two cases is shown in Fig. 8. We get a moment of inertia of the PNS corresponding to PSR J0348+0432 of 1.559×10^{45}g·cm^2 with σ^* and ϕ, and 1.510×10^{45}g·cm^2 without σ^* and ϕ. This indicates that including σ^* and ϕ in the PNS PSR J0348+0432 will increase the moment of inertia, explained by the bigger radius calculated above.

Likewise, the profile of surface gravitational redshift in a massive PNS for the two cases is shown in Fig. 9. We find that the gravitational redshift of the PNS corresponding to PSR J0348+0432 is 0.3701 when considering σ^* and ϕ, and 0.3747 without considering σ^* and ϕ. This result tells us that σ^* and ϕ in PNS PSR J0348+0432

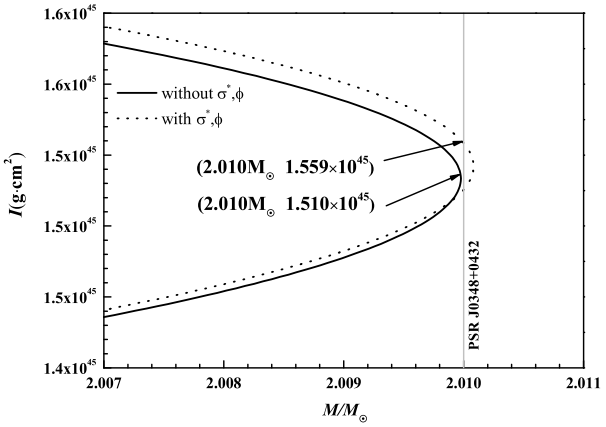

Fig. 8. The moment of inertia as a function of mass with and without considering σ* and ϕ. The shaded line corresponds to the PNS PSR J0348+0432.

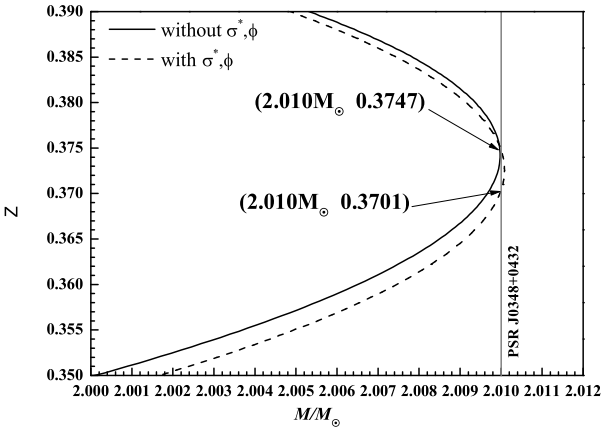

Fig. 9. The surface gravitational redshift as a function of mass with and without considering σ* and ϕ. The shaded line corresponds to the PNS PSR J0348+0432.

Table 6. The properties of PNS PSR J0348+0432 with and without considering σ* and ϕ. CASE1 considers σ* and ϕ, and CASE2 does not. R is the radius, I is the moment of inertia, and Z indicates surface gravitational redshift.

	$M_{\max}(M_\odot)$	R/km	I/(g· cm^3)	Z
CASE1	2.010	12.6520	1.559×10^{45}	0.3701
CASE2	2.010	12.6170	1.510×10^{45}	0.3747

will decrease the gravitational redshift. This is explained by the bigger radius giving smaller gravitational redshift, by the formula above.

All of these results are summarised in Table 6.

5 Summary

This paper discusses the influence of σ* and ϕ on the PNS PSR J0348+0432 in the framework of RMFT. We restrict the value of x_ω to a narrow range in the nucleon coupling sets GL85 and GL97, and we also exclude the possibility that GL97 could describe the PNS PSR J0348+0432. In the context of the GL85 set, we give two sets of hyperon coupling constants to describe the PNS PSR J0348+0432 with and without considering σ* and ϕ. We use an entropy per baryon of S=1 to emphasize the thermal effect on PSR J0348+0432 in this work, and study the different effects with and without considering σ* and ϕ. These effects include the particle number distribution, the mass-radius relation, the moment of inertia and surface gravitational redshift. We find that the PNS PSR J0348+0432 with σ* and ϕ will push forward the threshold for the appearance of hyperons. We find the mass-radius relations to be ($2.010M_\odot$, 12.6520 km) and ($2.010M_\odot$, 12.6170 km) corresponding to the PNS PSR J0348+0432 with and without considering σ* and ϕ, respectively. It means that the σ* and ϕ are in favor of increasing radius. The moment of inertia corresponding to the PNS PSR J0348+0432 are ($2.010M_\odot$, 1.510×10^{45}g·cm^2) and ($2.010M_\odot$, 1.559×10^{45}g·cm^2) respectively, the surface gravitational redshift corresponding to the PNS PSR J0348+0432 are ($2.010M_\odot$, 0.3747) and ($2.010M_\odot$, 0.3701) respectively. These calculations tell us that for σ* and ϕ in the PNS PSR J0348+0432, the redshift will decrease while the moment of inertia will increase, but there is no discernible difference between the changes. These conclusions indicate that the σ* and ϕ have very little influence on PNS PSR J0348+0432, which means that the restriction of σ* and ϕ on the interactions between baryons plays only a minor role in the PNS core.

The calculations and conclusions described above for a proto-neutron star of $2.01M_\odot$ could also be extrapolated to study other proto-neutron stars whose mass exceeds $2M_\odot$.

References

1 B. P. Abbott et al, Phys. Rev. Lett., **119**: 161101 (2017)
2 D. A. Coulter, R. J. Foley, C. D. Kilpatrick, M. R. Drout, A. L. Piro, B. J. Shappee, M. R. Siebert, J. D. Simon, N. Ulloa, D. Kasen, B. F. Madore, A. Murguia-Berthier, Y.-C. Pan, J. X. Prochaska, E. Ramirez-Ruiz, A. Rest, and C. Rojas-Bravo, Science, **358**: 1556 (2017)
3 P. B. Demorest, T. Pennucci, and S. M. Ransom et al, Nature(London), **467**: 1081 (2010)
4 J. Antoniadis, P. C. C. Freire et al, Science, **340**: 448 (2013)
5 B. Hong, H. Y. Jia, X. L. Mu, and X. Zhou, Chin. Phys. C, **40**: 065101 (2016)
6 Prasanta Char and Sarmistha Banik, Phys. Rev. C, **90**: 015801

(2014)
7 Feryal Özel, Dimitrios Psaltis et al, Astrophys. J. Lett., **724**: L199-L202 (2010)
8 Z. Zhang, L. W. Chen, Phys. Rev. C, **94**: 064326 (2016)
9 Ritam Mallick, Phys. Rev. C, **87**: 025804 (2013)
10 Q. F. Xiang, W. Z. Jiang, D. R. Zhang, and R. Y. Yang, Phys. Rev. C, **89**: 025803 (2014)
11 L. Ang et al, Chin. phys, **16**: 1934 (2007)
12 J. Schaffner, C. B. Dover, A. Gal, C. Greiner, and H. Stöcker, Phys. Rev. Lett., **71**: 1328 (1993)
13 H. Zheng, L. W. Chen, Phys. Rev. D, **85**: 043013 (2012)
14 S. Gandolfi, J. Carlson, and Sanjay Reddy, Phys. Rev. C, **85**: 032801 (2012)
15 Y. Sugahara, H. Toki, Nucl. Phys. A, **579**: 557 (1994)
16 X. F. Zhao, Phys. Rev. C, **92**: 055802 (2015)
17 Norman K. Glendenning, Phys. Rev. C, **23**: 2757 (1981)
18 M. M. Sharma, M. A. Nagarajan, P. Ring, Phys. Lett. B, **312**: 377 (1993)
19 W. Koepf, M. M. Sharma, P. Ring, Nucl. Phys. A, **533**: 95 (1991)
20 Z. Z. Ren, Phys. Rev. C, **65**: 051304 (2002)
21 J. Boguta, A. R. Bodmer, Nucl. Phys. A, **292**: 413 (1977)
22 J. Schaffner, C. B. Dover, A. Gal, C. Greiner, D. J. Millener, and H. Stöcker, Ann. Phys., **235**: 35 (1994)
23 Madappa Prakash, Ignazio Bombaci, Manju Prakash, Paul J. Ellis, James M. Lattimer, and Roland Knorren, Phys. Reps., **280**: 1 (1997)
24 J. R. Oppenheimer, and G. M. Volkoff, Phys. Rev., **55**: 374 (1939)
25 F. J. Fattoyev, and J. Piekarewicz, Phys. Rev. C, **82**: 025810 (2010)
26 Lee Lindblom, Astrophys. J., **278**: 364 (1984)
27 Benjamin D. Lackey, Mohit Nayyar, and Benjamin J. Owen, Phys. Rev. D, **73**: 024021 (2006)
28 N. K. Glendenning, Astrophys. J., **293**: 470 (1985)
29 S. Weissenborn, D. Chatterjee, and J. Schaffner-Bielich, Nucl. Phys. A, **881**: 62 (2012)
30 D. J. Millener, C. B. Dover, and A. Gal, Phys. Rev. C, **38**: 2700 (1988)
31 J. Schaffner, C. Greiner, and H. Stöcker, Phys. Rev. C, **46**: 322 (1992)
32 C. J. Batty, E. Friedman, and A. Gal, Phys. Reps., **287**: 385 (1997)
33 J. Schaffner-Bielich, A. Gal, Phys. Rev. C, **62**: 034311 (2000)
34 S. Aoki, S. Y. Bahk, K. S. Chung et al, Phys. Lett. B, **355**: 45 (1995)
35 P. Khaustov, D. E. Alburger et al, Phys. Rev. C, **61**: 054603 (2000)
36 N. K. Glendenning and S. A. Moszkowski, Phys. Rev. Lett., **67**: 2414 (1991)
37 S. Pal, M. Hanauske, I. Zakout, H. Stöcker, and W. Greiner, Phys. Rev. C, **60**: 015802 (1999)
38 X. L. Mu, H. Y. Jia, X. Zhou, and H. Wang, Astrophys. J, **846**: 140 (2017)